TOWARDS FIELD MEASUREMENTS OF POPULATIONS OF METHANE GAS BUBBLES IN MARINE SEDIMENT: AN INVERSION METHOD REQUIRED FOR INTERPRETING TWO-FREQUENCY INSONIFICATION DATA FROM SEDIMENT CONTAINING GAS BUBBLES

TIMOTHY LEIGHTON[1], AGNI MANTOUKA[1], PAUL WHITE[1], ZYGMUNT KLUSEK[2]

[1] Institute of Sound and Vibration Research, University of Southampton,
Highfield, Southampton SO17 1BJ, UK
tgl@soton.ac.uk

[3] Institute of Oceanography, Polish Academy of Sciences,
Sopot, P.O. Box 148, Poland

This paper describes a key stage in the process for developing a new device for the measurement of gas bubbles in sediment. The device is designed to measure gas bubble populations within the top 2 m of marine sediments, and has been deployed at inter-tidal sites along the South coast of England. Acoustic techniques are particularly attractive for such purposes because they can be minimally invasive. However they suffer from the limitation that their results can be ambiguous. Therefore it is good practice to deploy more than one acoustic technique at a time. The new device does just this, but it is designed with the practical economy that the task is accomplished with the minimum number of transducers. One of the measurement techniques relies on insonifying the sediment with two frequencies. This paper outlines how the bubble size distribution is inferred through inversion of the signals detected when two frequencies are projected into the sediment. The high attenuation of the sediment makes this interpretation far more difficult than it would be in water. This paper outlines these difficulties and describes how they can be overcome.

INTRODUCTION

A new device has been designed to measure gas bubble populations within the top 2 m of marine sediments, and has been deployed at inter-tidal sites along the South coast of England. Acoustic techniques are particularly attractive for such purposes because, unlike the acquisition of core samples, they are non-invasive (apart from any effect the sound field itself might have on the bubble population [1], or unintended disturbance of the site by the physical presence of the transducers and supports). However they provide ambiguous results, since for almost all acoustic bubble detection techniques, more than one type of acoustic bubble interaction can generate the signal under consideration [2]. Care is therefore required in performing the acoustic inversion which estimates the bubble size distribution. This paper describes the considerations required for inverting two-frequency information from gassy sediment.

Populations of bubbles (mainly methane) occur at many locations [3, 4], and the ability to make such measurements is of increasing interest [5-37]. This is, first, because of the impact those bubbles have on the structural integrity and load-bearing capabilities of the sediment [38, 39]; second, because the presence of bubbles can be indicative of a range of biological, chemical or geophysical processes (such as the climatologically-important flux of methane from the seabed to the atmosphere) [40]; and third, because of the effect which the bubbles have on any acoustic systems used to characterise the sediment.

There exist several options for measuring the populations of gas bubbles in sediment, each with their commensurate advantages and disadvantages. Many of these techniques are limited in terms of what can be deployed in the field, the invasiveness of the technique (in terms of disturbing the sample that is being measured), and the compromise between the side-effect that the 'field of view' (or equivalent) tends to decrease as the 'magnification' is increased to decrease the minimum size of bubble that can be detected. The latter is particularly critical with marine bubble populations, where sample volumes of the order of 1 m^3 may be required for a statistically significant sample, a volume which can contain tends of millions of micron-sized bubbles [41]. The use of CT scanning of cored sample is a particularly direct method (Figures 1 and 2), although acquisition, transport and storage of the core can disturb the sample to a greater or lesser extent.

Acoustic techniques can suffer less than many of the alternatives with respect to these criteria. However unlike optical or other techniques based on EM-signals, acoustic measurements tend to be indirect. As such, there is often an inherent ambiguity in any acoustic measurement of a bubble population, and as a result it is often good practice to deploy more than one acoustic technique [2, 42-44]. In this way, the limitations of one method may be compensated for in the deployment of another, and a measured population may be validated through comparison with an independent measurement of the same population, or one closely-related in time and space to the first population [2, 43-46]. One combination of techniques that has proven to be particularly promising is that of attenuation along an array with a combination-frequency system, since this is efficient in the number of transducers it deploys, and brings together complementary linear and nonlinear aspects with which to interrogate the bubble population [47, 48]. The linear aspect is represented in the apparatus by the so-called 'attenuation' technique, which involves inversion of the measured attenuation and sound speed as a sequence of tones (or an appropriate alternative signal) propagates along a hydrophone array. Whilst this is a familiar technique for use in water, an appropriate model for propagation in gassy sediments needs to be developed for it to be applied there [34].

Figure 1. Image generated through CT scanning of a vertical core through bubbly gel (described in reference [49]), used for validation purposes during the construction of the device described in this paper. In the image, the host gel near the edges of the quadrant has been clipped back to show the presence of the bubbles. For scale, the largest bubble visible has a diameter of ~ 1mm.

The nonlinear aspect of the new device is represented by the 'two frequency' technique. In the past, two-frequency insonification of bubbles has been used successfully to determine bubble size distributions in water [50, 51]. This appears in two forms [52]: if the two frequencies are close together, it is usually assumed that the scattering at the difference frequency is due to bubbles which are resonant at that difference frequency. This is termed the 'combination frequency' technique. However if one frequency (the 'imaging' frequency) is very much higher than the other (the 'pump' frequency), then scattering at the difference frequency is taken to be due to bubbles which are resonant at the pump frequency. This is termed the 'modulation frequency' technique [52].

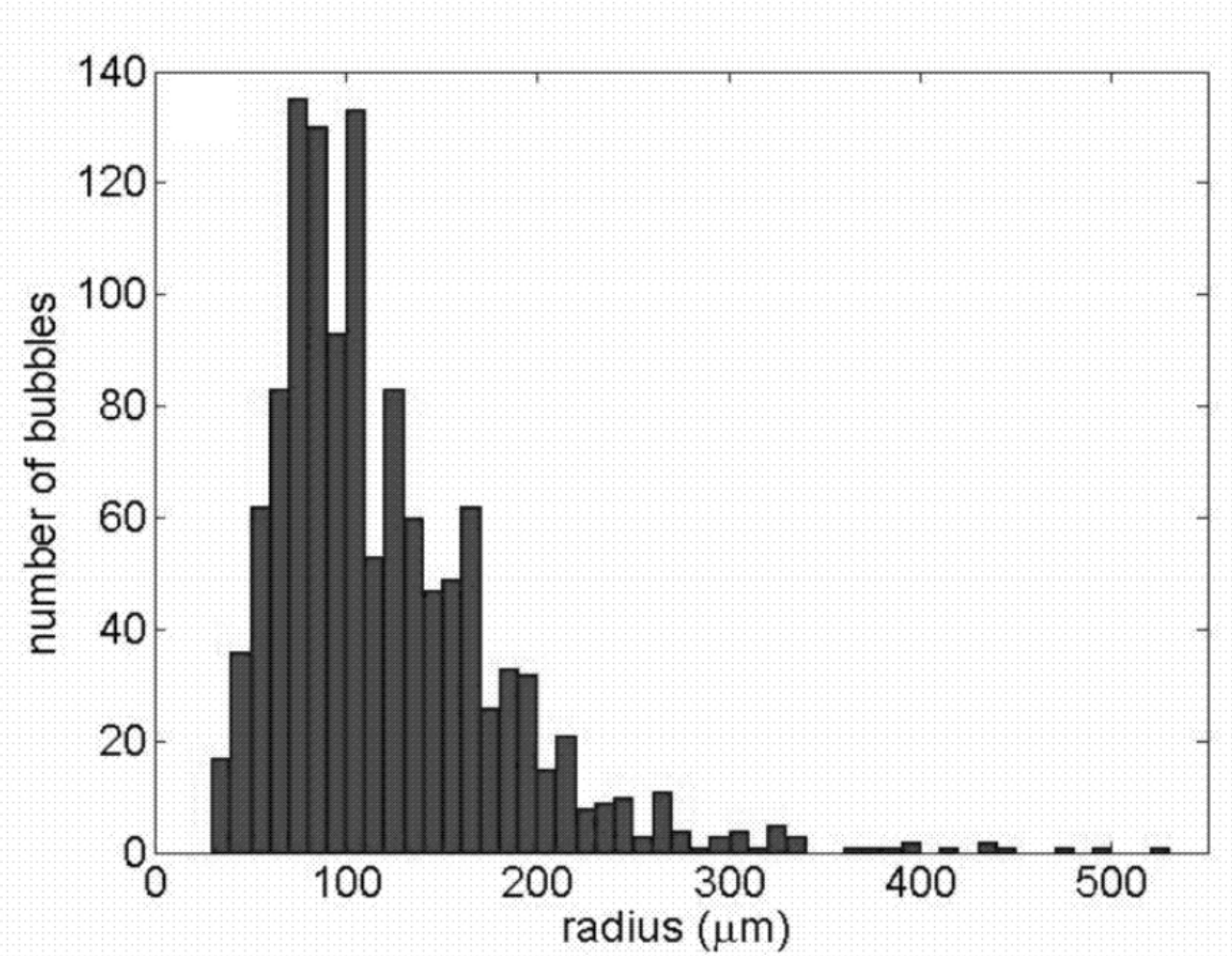

Figure 2. The combined bubble size distribution obtained from the sample shown in Figure 1 (including those bubbles which cannot be seen because they are within the opaque host gel) and two other samples. See reference [49] for details.

These common and simple assumptions will now be tested through simulation to determine their validity for use in water. This critical analysis is required, because the paper then tests how the same assumptions perform when the bubbles are present in sediment. There are two differences with sediment which need to be taken into account. The first, which will not be tested in this paper but rather investigated in a later paper, involves the results of using a model which properly reflects the different dynamics in sediment as opposed to water: the required model is currently under development [34] (and is also required for inversion of the 'linear' technique, described above). The second difference is a practical one, and arises because of the likely circumstance that, in gassy marine sediments, the attenuation will be so great at high frequencies that the 'imaging' signal cannot be at a frequency which is very much greater (say 2 orders of magnitude greater) than the frequency used for the 'pump' wave. As such, the simple assumptions employed when O(MHz) imaging frequencies are used in water no longer apply: the situation is neither that found in the limit of the 'combination frequency' technique or the 'modulation frequency' technique. In this 'mixed frequency' regime, more than one bubble interaction can generate the required signal, and the inversion must take this into account.

1. APPARATUS

The new device deploys two acoustic techniques and, after the cessation of the tests, a core sample is taken for CT analysis. For the 'attenuation' technique described in the previous section, compressional wave attenuations were measured from 30 kHz to 100 kHz through the analysis of propagation signals transmitted from a variety of sources to a buried co-linear hydrophone array. These attenuations are then inverted to estimate the bubble size distribution along the array. Until the development of the new model has been completed [34], these inversions currently treat the host medium as though it were water (future papers will describe how that deficiency is removed). In addition 'two frequency' system (the one which is described as representing nonlinear techniques in the preceding section) provides a second estimation of the bubble population. One of the two frequencies is the same as that used in the 'attenuation' technique, so that the device makes economic savings by using the transducer responsible for that wave for two purposes (and indeed the wave can in principle be used for both purposes simultaneously, although that is not done here for practical deployment purposes). This signal ranges from 30 to 100 kHz, and interacts with a second acoustic field (fixed at 220 kHz).

Although this paper will not report any new developments in the 'attenuation technique', it is useful to consider how this technique has evolved. This is because the 'two-frequency technique' is currently at a similar stage to that occupied by the 'attenuation' technique in the 1980s, and needs to undergo a similar process of evolution.

Over the past few decades, the inversion by which the bubble population is inferred in the 'attenuation' technique has evolved from a stage, in the 1980s, when only resonant bubbles were considered to be responsible for attenuation. The hardware associated with the method of estimating bubble populations from the effect that those bubbles have on the attenuation (and sometimes sound speed) of the measured signal as it propagates along an array, has barely changed over the decades since it was introduced (except for increases in bandwidth and array size) [52-63]. What has changed is the sophistication of the algorithm used to infer the bubble population from the measured attenuation: the earliest interpretations assumed that only resonant bubbles contributed [54, 64], whilst later methods included the contribution of off-resonant bubbles [65] and later still the analysis was adapted to account for the nonlinear effects that will

occur when high acoustic pressures are used to ensure adequate signal-to-noise ratios despite large attenuations [66]. Furthermore there has been a recognition that this technique can give misleading results if only a single receiver is used, as bubble-induced variations in sound-speed, beam pattern etc. (particularly in the near field) can be misinterpreted as contributions to bubble-induced attenuation [67].

It is now timely to ask whether a similar evolution is required in the sophistication given to the interpretation of the signals from two-frequency insonification, which has traditionally relied on the assumption that only one type of bubble motion at a time is responsible for the detected nonlinear frequency generation.

The estimation of bubble populations from two-frequency insonification tends to fall into two distinct categories, although both are associated with quadratic nonlinearities terms in the bubble pulsation [68-82]. In the first, the bubbles are driven at two frequencies which are close together, and the signal at the different frequency is, to first order, taken to arise at bubbles whose pulsation resonances occur at that difference frequency. This will here be termed the 'combination-frequency' technique, as described above [83]. Alternatively, in the 'modulation frequency' technique, one of the sources is assumed to drive the bubbles to pulsate at the 'pump' frequency', whilst a much higher 'imaging frequency' is scattered from the bubbles: that component of the imaging frequency which is modulated at the pump frequency is interpreted as arising through scatter of the imaging frequency off bubbles which are resonant at the pump frequency [84]. It is more difficult to realize this latter idealized situation in the sediment than it is in the water column, since the attenuations in the gassy seabed as so high as to preclude using a very high imaging frequency, which may tend to be closer to the pump frequency than the idealized explanation above implies. Hence in the sediment, the interpretation of the generation of scattered spectra in response to two-frequency insonification of a bubble population will require a modeling of how all of the bubbles in that population respond to whatever two frequencies are incident upon them, rather than the simple idealized distinction and explanation given above.

2. SIMULATION OF SCATTERING FROM SINGLE BUBBLES

Simulations were undertaken using the Rayleigh-Plesset equation with enhanced viscosity for the pulsations of air bubbles in water when insonifed by two primary fields of frequencies f_1 and f_2:

$$(\ddot{x}+\ddot{x}x)+1.5\dot{x}^2+\omega_0^2 x-(1/\rho_0 R_0^2)\left(1.5\kappa\left(3\kappa+1\right)\left(p_0+2\sigma/R_0\right)-2\sigma/R_0\right)x^2 \qquad (1)$$
$$+2\beta_{tot}(\dot{x}+x\dot{x})=-(1/\rho_0 R_0^2)P(t).$$

where x is the normalised perturbation of the time-dependent bubble radius R about the equilibrium value R_0:

$$R=R_0(1+x). \qquad (2)$$

In equation (1), the undamped natural frequency for bubble pulsations is

$$\omega_0 = \sqrt{(3\kappa(p_0 + 2\sigma / R_0) - 2\sigma / R_0) / \rho_0 R_0^2} \tag{3}$$

where ρ_0 is the equilibrium liquid density, κ is the polytropic index of the gas, p_0 is the static pressure in the liquid at the bubble wall, and σ is the surface tension on the bubble wall. In equation (1), the driving pressure field is:

$$P(t) = P_1 \cos(2\pi f_1 t) + P_2 \cos(2\pi f_2 t) \tag{4}$$

The absorption coefficients accounting for the viscous, radiation and thermal loss mechanisms (β_{vis} β_{rad} , β_{th}) are added together to form a total equivalent coefficient β_{tot} that accounts for all losses [85, 86]:

$$\beta_{tot} = \beta_{vis} + \beta_{rad} + \beta_{th} \ . \tag{5}$$

The losses resulting from acoustic radiation and thermal dissipation are incorporated by a linear enhancement of β_{tot}, such that the viscous loss coefficient is:

$$\beta_{vis} = \frac{2\mu}{\rho_0 R_0^2} \ . \tag{6}$$

where μ is the shear viscosity of the liquid. The radiation loss coefficient is:

$$\beta_{rad} = \frac{\omega^2 \cdot R_0}{2c_0} \ . \tag{7}$$

where c_0 is the sound speed in the liquid in the linear limit. The 'driving frequency' ω is simple to interpret when the bubble is oscillating in steady state in response to single-frequency driving, but for two-frequency insonification we will use the frequency which contains the most energy when the wall pulsation time history in the steady state is spectrally analysed. The linearized thermal loss coefficient is:

$$\beta_{th} = \frac{p_o}{2\rho_0 \cdot \omega \cdot R_0^2} \mathrm{Im}\,\Phi \ . \tag{8}$$

The complex function Φ depends on the D_g thermal diffusivity of gas bubble through the parameter X [58]:

$$X = \frac{D_g}{\omega \cdot R_0^2} \ . \tag{9}$$

(a)

(b)

(c)

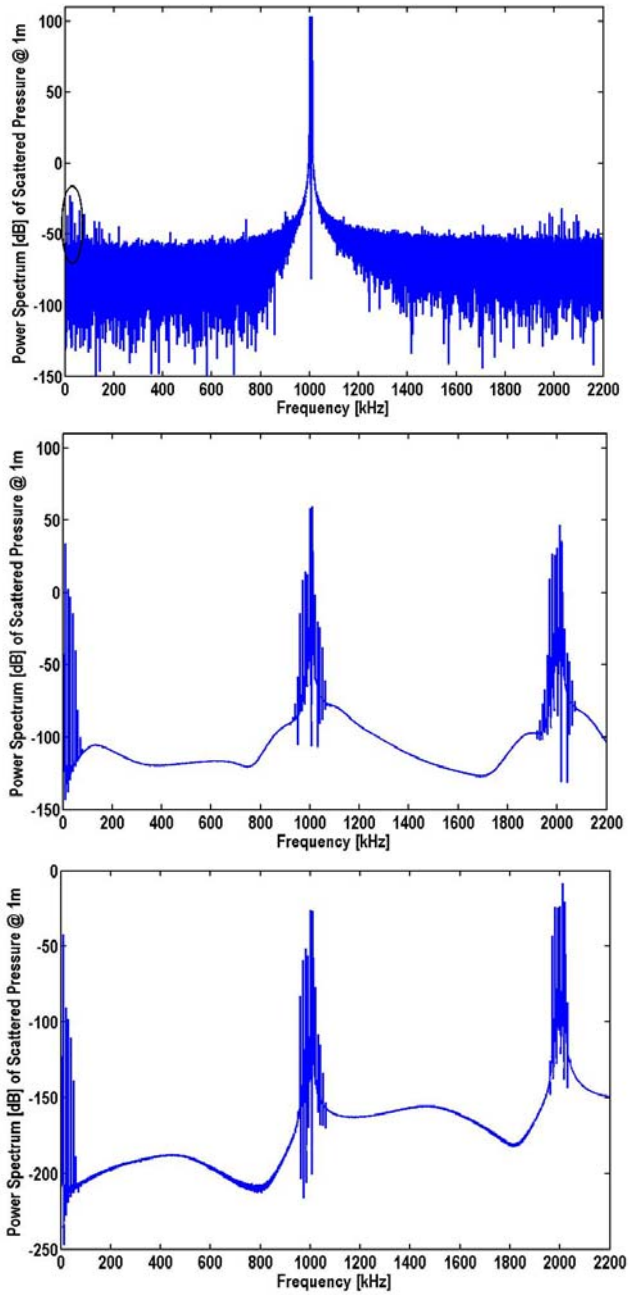

Figure 3. Power spectra (with a common dB normalisation) of scattered pressure form a single bubble of size resonant at: (a) $f_2 - f_1$ =10 kHz (the 10 kHz peak is circled), (b) f_1 =1 MHz and (c) $f_2 + f_1$ = 2.01 MHz. Both waves have 15 kPa 0-peak pressure amplitudes.

The first simulation set examines the assumptions of the 'combination-frequency' technique using numerical solutions of equation (1) using Matlab ode45 solver: A single air bubble was assumed to undergo small amplitude pulsations in fresh water of 14°C, at a depth of 2 meters under a two frequency insonification. Both acoustic waves have pressure amplitudes of 15 kPa

(0-peak amplitude). Figure 3 shows the predicted power spectra of the pressure scattered at one meter using the equation when insonification by a frequency f_1=1 MHz and f_2 = 1.01 MHz. For these predictions the bubble was assumed to emit as a monopole source according to:

$$P(r,t') = \frac{\rho_0}{r}\left(2R\dot{R}^2 + R^2\ddot{R}\right), \tag{10}$$

where t' denotes the retarded time and r the radial distance from the bubble centre. It is recognised (see Section 3) that, in fact, a form factor may be required to account for non-monopole scattering from larger bubbles [87], but for this simple demonstration monopole scattering will be assumed for all bubble sizes. In the simulations of figure 3 the bubble sizes are selected such that the bubble is resonant at: (a) $f_2 - f_1$=10 kHz, i.e. $R_0 \approx 350\ \mu$m, (b) f_1 and f_2 i.e. $R_0 \approx 3.5\ \mu$m, and (c) $f_2 + f_1$=2.01 MHz, i.e. $R_0 \approx 1.75\ \mu$m. This tests the 'combination' frequency assumption that only bubbles resonant at the difference frequency are contributing to the scattered signal. As already revealed from previous works [88], there is a monotonic relationship between the scattered pressure and the bubble size only when the bubbles which are resonant at the insonification frequencies are neglected. Figure 3 shows that the signal at the difference frequency is much stronger when bubbles are resonant with the frequency of the primary field (Figure 3 (b)) than when bubbles are resonant with the difference frequency (Figure 3(a)), whereas resonances at the sum of the primary field give a negligible signal (Figure 3(c)). Therefore this technique requires very high insonification frequencies and an *a priori* knowledge that very small bubbles (order of magnitude of a few of microns) are not present.

The second set of simulations (Figure 4) shows the scattered pressure spectra of a single bubble under a set of insonification frequencies used for the apparatus described in this paper: f_1=30 kHz and f_2 = 220 kHz. The field pressures and the simulation conditions are the same as the ones used for the simulations of the first set. As opposed to the first simulation set, here the bubble sizes resonant at each of the primary frequencies are distinguishable. The simulations of Figure 4 show the scattered power spectra for bubble sizes resonant at: (a) $f_2 - f_1$=190 kHz, i.e. $R_0 \approx 18.5\ \mu$m, (b) f_1=30 kHz i.e. $R_0 \approx 116\ \mu$m, (c) f_2= 220 kHz i.e. $R_0 \approx 16\ \mu$m, and (c) $f_2 + f_1$=250 kHz, i.e. $R_0 \approx 14\ \mu$m.

The numerical simulations of bubble dynamics for this type of insonification lead to the generation of a series of harmonics and combination frequencies between the pump and the imaging frequency (e.g. $2f_1$, $2f_2$, $f_2 - f_1$, $f_2 + f_1$, $f_2 - 2f_1$, $f_2 + 2f_1$ etc. [89]). Hence the technique is actually neither of the idealized types, i.e. it is neither purely 'combination-' nor 'modulation-' frequency, but rather is a 'mixed-frequency' method. As shown in Figure 4, if a range of bubble sizes is present in the bubble population, there is no simple one-to-one mapping between a single bubble size and the energy scattered at a single frequency. For example, the single bubble that is resonant at the difference frequency (Figure 4(a)) does not overwhelmingly dominate the detected signal, compared to, say, the scattering from a resonant bubble at the pump or imaging frequencies or even at the sum frequency. No monotonic relationship between the difference frequency and the resonant bubbles exists. However, even in such circumstances, an inversion can still carried out by monitoring the difference frequency, as the following section explains.

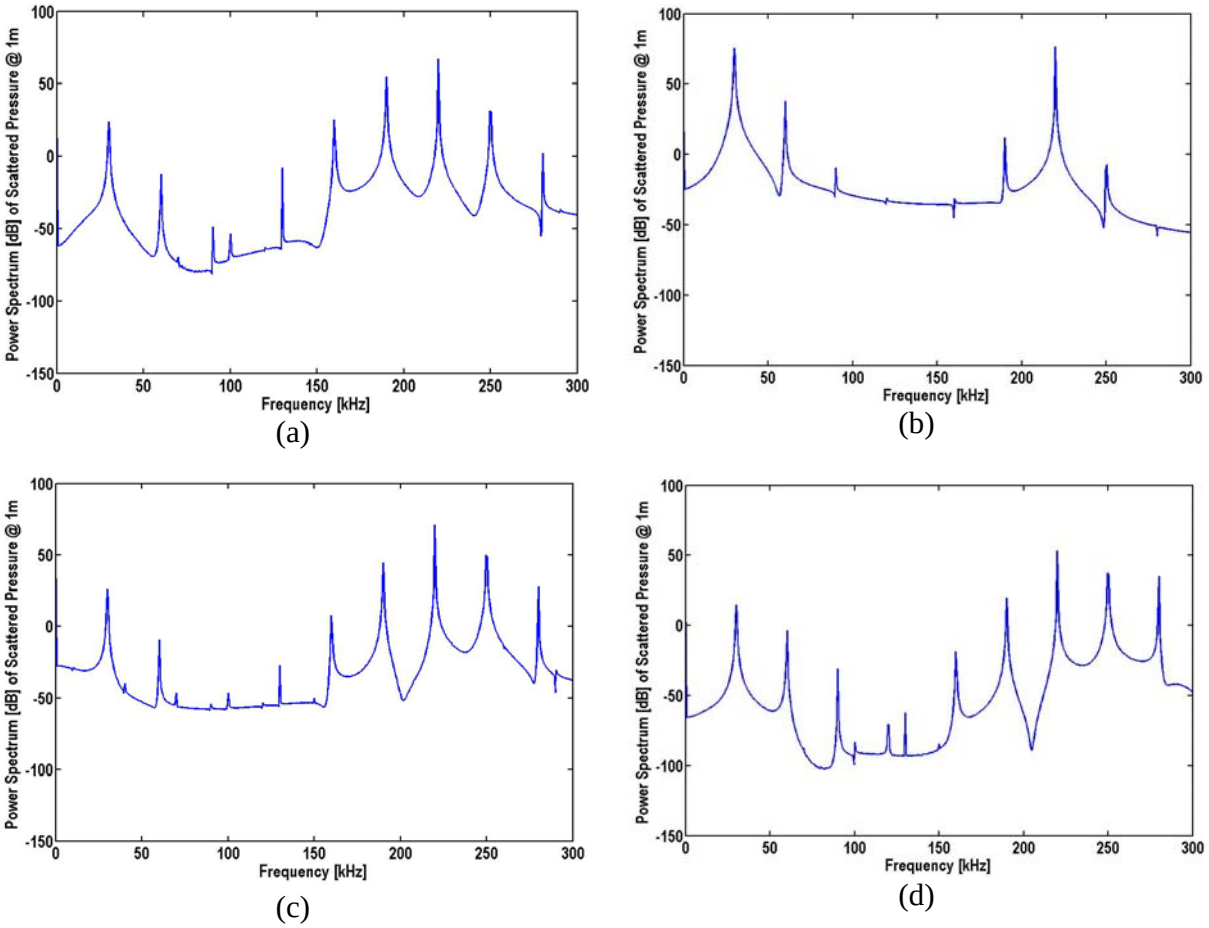

Figure 4. Power spectrum (with a common dB reference) of scattered pressure form a single bubble of size resonant at (a) $f_2 - f_1$ =190 kHz, (b) f_1 =30 kHz (c) f_2 =220 kHz and (d) $f_2 + f_1$ = 250 kHz. Both waves have pressure amplitude of 15 kPa (0-peak).

3. THE INVERSION

An inversion was carried out using the 'mixed- frequency' method by predicting the emitted pressure from all the possible bubble sizes present in the insonification volume. The predictions were for every frequency pair used for the experiments, with the simulations described at the previous section. Using these predictions the difference frequency pressure spectral component was monitored and stored in a matrix. This is explained further in the next paragraph.

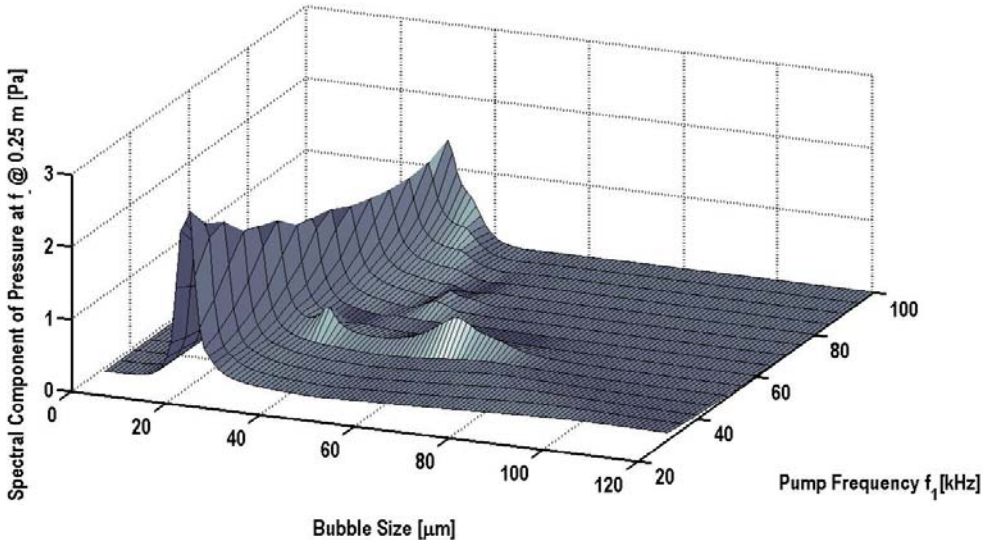

Figure 5. Three dimensional representation of the inversion matrix corresponding to the tank experiments undertaken with the 'mixed-frequency' device. The pressure emitted at difference frequency (vertical axis) was computed for bubble sizes ranging form 1 to 120 micron using one micron bins and for pump frequencies ranging from 30 kHz to 100 kHz with increments of 5 kHz.

For the experiment described in this paper to test the 'mixed-frequency' device, the first insonification frequency (f_1, the pump frequency) varies from 30 to 100 kHz in 5 kHz increments whereas the second (f_2, the imaging frequency) was kept constant at 220 kHz. Both pressure signals have amplitudes (0-to-peak) of 15 kPa at the centre of the region where the two primary beams intersect with each other. This region is common with the receiver sensing volume and that intersection point is 0.25 m distant from the receiver's surface (see Figure 6; more details will follow when the device is described in Section 4). Assuming monopole scattering (see below), under these conditions the scatter at difference-frequency was computed for bubble sizes from 1 to 120 micron with 1 micron increments i.e. 1 micron bins. This leads is a matrix formulation: each row of this matrix gives the contribution of each bubble bin size at the difference frequency under consideration whereas each column of this matrix gives the importance of a certain bubble size for the difference frequencies ($f_2 - f_1$) used in the experiments. A three dimensional representation of this matrix is shown in Figure 5 using linear

axes in all dimensions. The vertical axis shows the scattered pressure from a single bubble, whereas every point of the grid of the horizontal plane represents the bubble size/pump frequency combinations for which the computations were carried out. Hence the surface represents the weighting factors for the inversion.

As shown in Figure 5, there is not a one-to-one mapping between the difference-frequency spectral component and the bubble size for every pump frequency. Although greater peaks occur for bubble sizes resonant at the difference frequency $f_2 - f_1$ (these peaks form the backbone of the curve) the other peaks cannot be ignored for the inversion as they have the same order of magnitude.

It is worth commenting on the potential for compromising the assumption of monopole radiation. The largest bubble in the inversion has a radius of $R_0 \approx 100\ \mu\text{m}$. The highest frequency of relevance to the simulation would be the sum frequency 220 kHz + 100 kHz, although in fact if (as is the case here) the highest frequency involved in inverting the difference frequency to obtain bubble size in formation would be 220 kHz – 30 kHz = 190 kHz. Depending on the exact value used for c_0, the speed of sound in gassy sediment at the frequency in question, this gives the largest values of $\omega R_0 / c_0$ to be less than 0.2. Because of this, the monopole assumption is used in this first attempt at an inversion. This is one way in which the low value of the imaging frequency is advantageous in sediment. Of course, it is highly likely that bubbles larger than $R_0 \approx 116\ \mu\text{m}$ (the size resonant with the lowest pump frequency) are present in the population, and this has serious consequences when considering the inversion based on the 'attenuation' method [67]. However the implications for the two-frequency technique are perhaps not so serious, as such bubbles will not pulsate and will therefore not contribute to the generation of any nonlinearities. If of course the lowest pump frequency were to be reduced such that significant departures from monopole scattering are seen, then correction for this not difficult because the orientation of the high frequency receiver and transmitter are fixed, so that the scattering angle is well known, as described by Phelps and Leighton [87]. One might worry that, since the lower imaging frequency takes us out of the realm of the idealized 'modulation-frequency' model then the direction of the incident beam cannot be rigorously identified with the direction of the imaging field, but the fact that the pump has been lowered to take us out of the monopole scattering regime self-corrects for this.

4. TANK TESTS: MEASUREMENTS

The apparatus for the 'mixed-frequency' technique is shown in Figure 6. The high frequency transmitter and receiver (A and C in the photograph) have a common focus point where their acoustic axes intersect each other at 90°, their axes being 45° either side of the axis of the pump transmitter (which is also the axis of symmetry of the device). The apparatus was tested in a fresh water tank with dimensions 8 m x 8 m x 5 m (deep) in order to test out the inversion procedures and cross-check these against other methods of measuring the bubble size distribution. Bubbly water was pumped via a hose at the bottom of the tank. The rig was placed horizontally at a depth of 2 m, and the bubbles allowed to rise through the measurement volume. The advantage of this configuration is that there is a small and well defined scattering volume for all pump frequencies using a frequency ranges suitable for sediments. It is practical for deployment of the instrumentation on the surface of the mud.

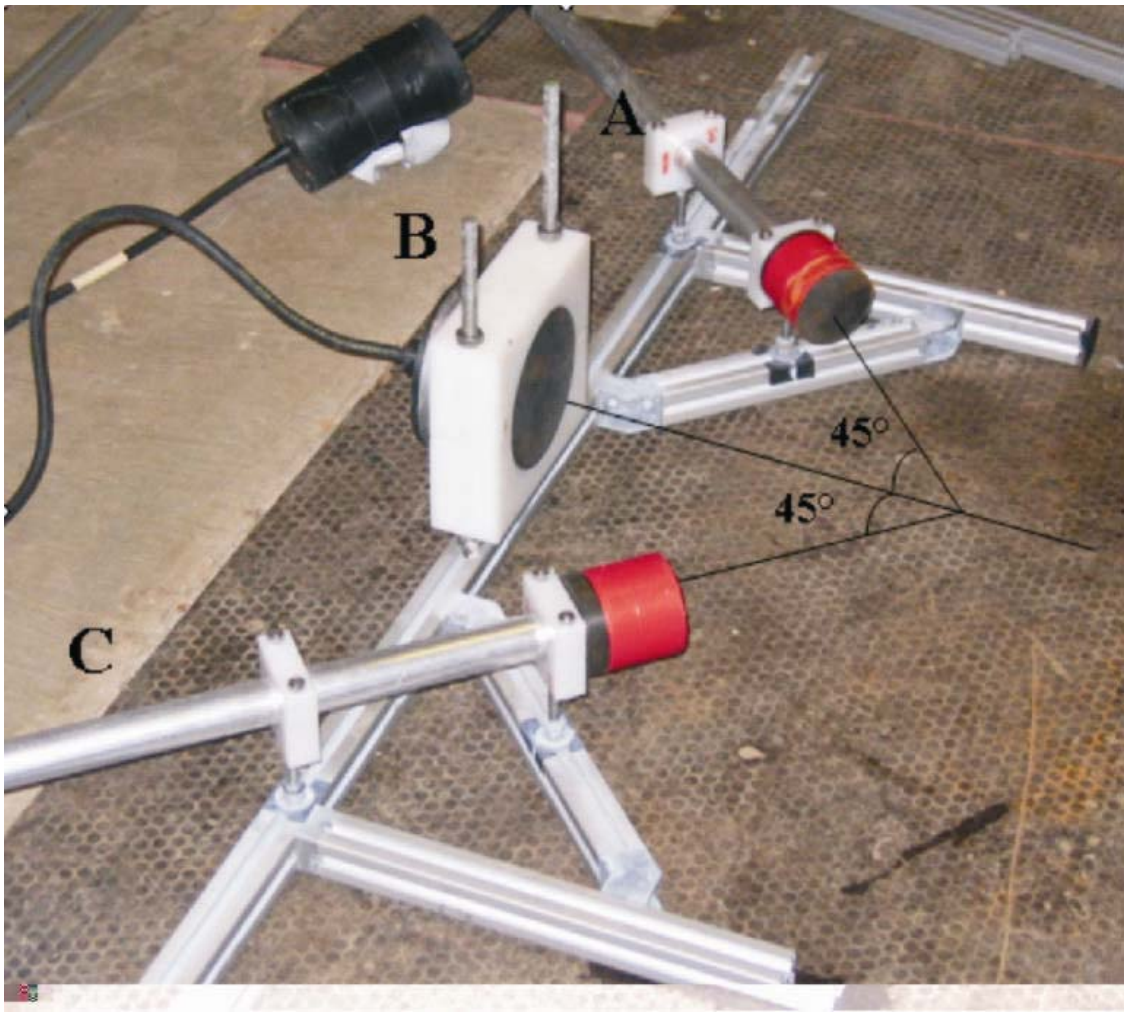

Figure 6. The combination-frequency apparatus: the three devices, the high (imaging) frequency transmitter (A) , the pump source (B) and the high (imaging) frequency receiver (C) are mounted on a rig so that the devices have a common focus point. The imager and the receiver have equal angular distances (45°) from the pump axis

It is important to calculate the size and location of the measurement volume because the bubble count needs to be converted to a bubble concentration, and therefore its volume needs to be known. This is defined by the 3 dB limits of the overlap of the f_2 imager field and the high frequency receiver. There are some subtleties in this. First, although the 3 dB overlap beam pattern may appear to be a somewhat arbitrary choice, it reflects the chosen 3 dB limit for the requirement placed on bubble to be counted as 'resonant' at a particular frequency.

Second, the sensing volume of this device, which is located in the far field of all transducers, changes with frequency. Whilst the beam pattern for the high frequency transmitter needs to be calculated at the imaging frequency, the relevant beam pattern of the receiver is that

which is calculated at $f_2 - f_1$. Beam pattern calculations computed the sensing volume to have a minimum value of $\sim 9 \times 10^{-6}\,\mathrm{m}^3$ and a maximum of $\sim 1.6 \times 10^{-5}\,\mathrm{m}^3$. Noting that error bars on bubble size distributions are typically much greater than this variation, for this first trial of this method of inversion, the calculations presented here use a 'typical' value of that volume ($10^{-5}\,\mathrm{m}^3$). It would however not be difficult to correct for the frequency-dependence of the sensing volume when the formal inversions are calculated in later papers.

(a)

(b)

(c)

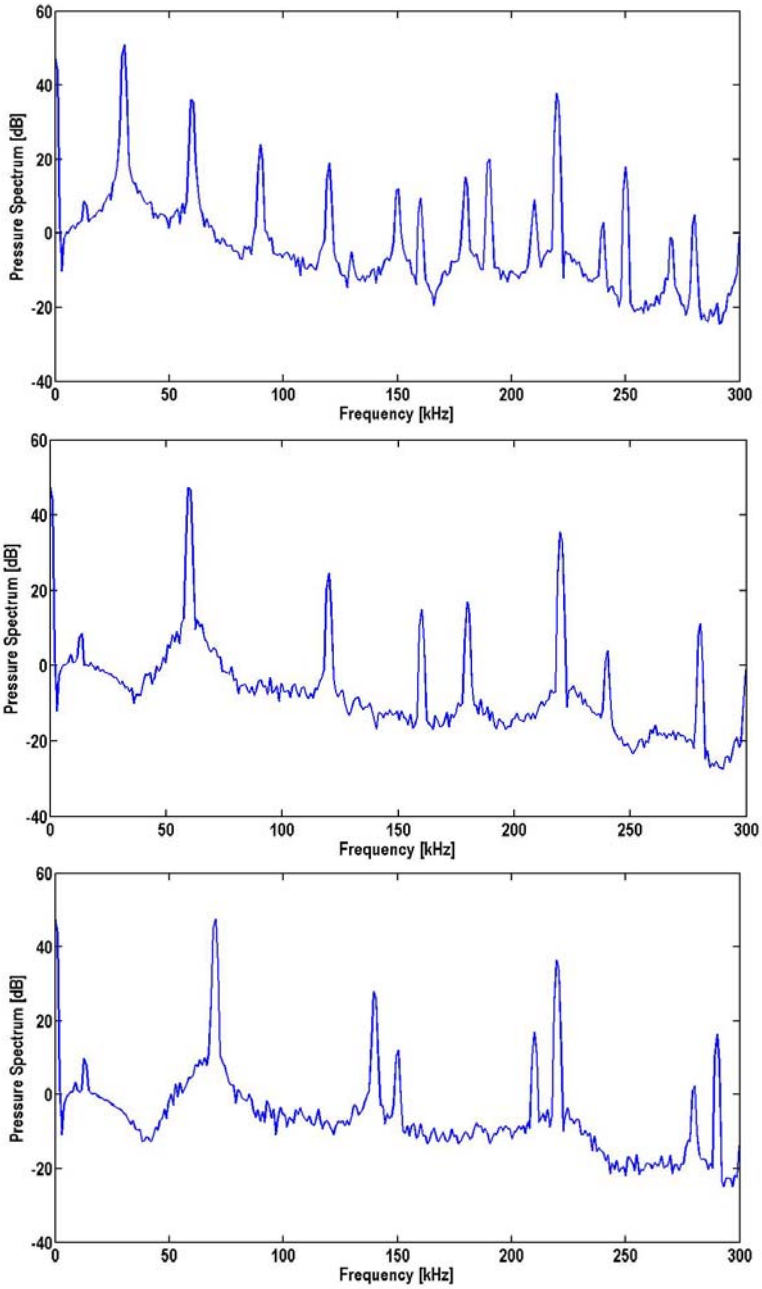

Figure 7 Mean-square spectra (with a common dB reference) of the measured pressure at the receiver, for imaging frequency of 220 kHz and pump frequency of (a) 30 kHz, (b) 60 kHz and (c) 70 kHz. Here spectral frequencies between 20 kHz and 310 kHz are shown.

5. TANK TESTS: RESULTS

For the first tank test with this device, the imaging frequency, f_1 was kept constant at 220 kHz and the pump frequency f_2 varied from 30 kHz to 100 kHz in increments of 5 kHz. The acoustic sources were adjusted such that, at focus point, the pressure was constant at 15 kPa (zero-to peak amplitude) for all frequencies. A 2 ms square pulse was generated for each combination frequency and the scattered signal was recorded using an acquisition card with a sampling frequency of 2 MHz. Figure 7 shows the mean spectrum obtained from two sets of 10 consecutive pulses for each a pump frequency of 30 kHz (Figure 7(a)), 60 kHz (Figure 7(b)) and 70 kHz (Figure 7(c)), when gas bubbles rose through the whole sensing volume.

As expected from the numerical simulations, many other nonlinear generated components exist between the pump and the imaging frequencies. However this is not a limitation for the inversion as long as the contribution to the difference-frequency spectral component generated by each size of bubble at each insonification pair is known (see graph in Figure 5). These contributions are weighting factors that reflect the amount of bubbles present with the certain bubble size. Multiplication of this matrix with the weighing factors with the measured pressure at the difference frequency (Figure 8) gives a first estimate of the bubble population present in the measurement volume (Figure 9). It should be noted, when considering this inversion, that this matrix is ill conditioned and therefore the results depend on the matrix regularisation. For the inversion shown in Figure 9, the matrix was inverted using the Moore-Penrose pseudoinverse method. The authors are currently undertaking studies to cross-validate these results with another inversion method.

The inversion was implemented assuming incoherent scattering although, owing to the device configuration, the pressure measured at the receiver is scattering with both coherent and incoherent parts [90]. Since the wavelength in bubble-free water at 220 kHz is around 7 mm, and the size of the dimensions of the measurement volume is 3-4 times greater, this assumption can give accurate results for experiments in water exhibiting a high variability of bubble concentration in time because the coherent part is averaged out when using many measurements for each insonification frequency. However in mud, this approach may not be applied because the bubbles are expected to have much less variability with the measurement time, and therefore a rather sophisticated algorithm has to be applied in order to correct for the coherent scattering. This will be explained in a later paper.

7. CONCLUSIONS

In this paper a 'mixed-frequency' nonlinear inversion method and the corresponding device are described. This method uses two acoustic frequencies which are suitable for application in sediments. The device is also designed for non invasive field measurements. Here the first tests in a water tank with air bubbles were presented; followed by an inversion of bubble population. These results proved the feasibility of this new method.

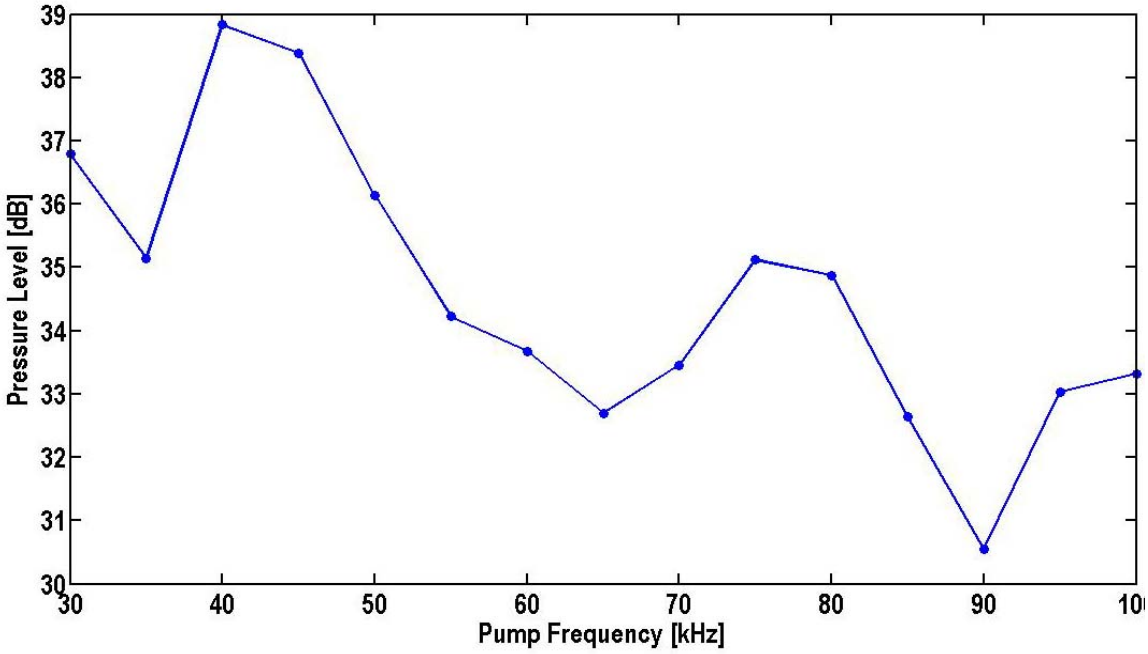

Figure 8. Spectral level of the pressure signal at the difference frequency (as measured at the receiver and expressed on a dB scale), plotted at a function of the varying pump frequency.

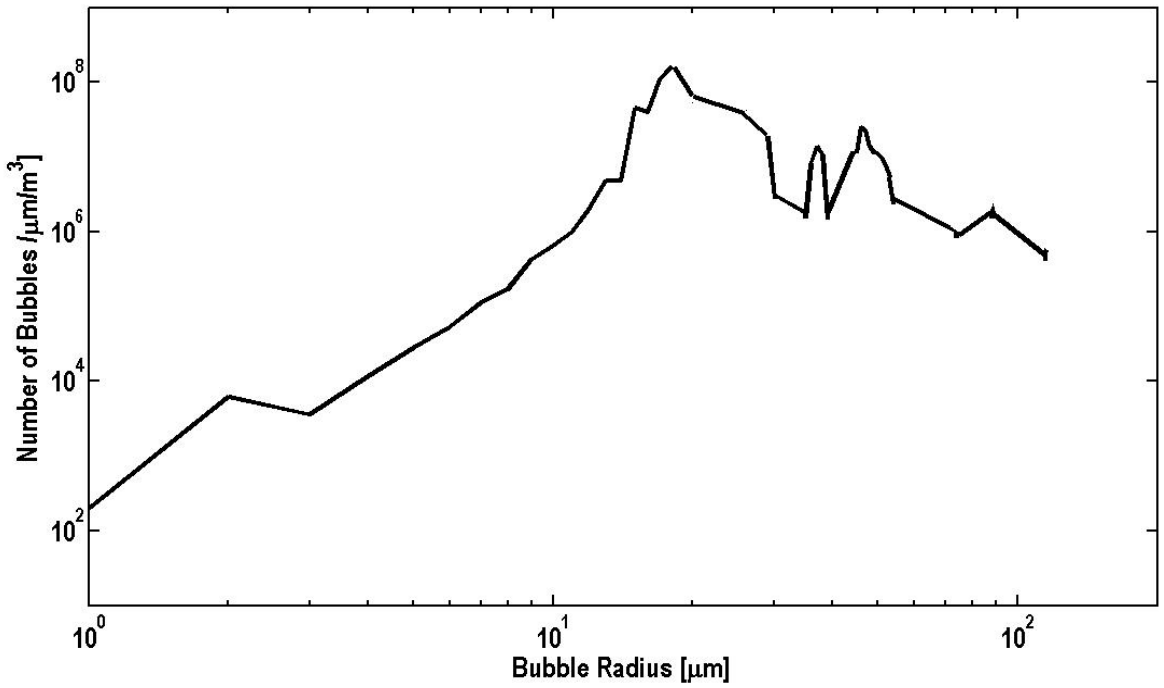

Figure 9. An estimate of the number of bubbles per cubic metre of bubbly water, per micron radius bin, is plotted as function of bubble radius inferred from the tank measurements.

8. ACKNOWLEDGEMENTS

This work has been funded by the UK Engineering and Physical Sciences Research Council (Grant number EP/D000580/1; T. G. Leighton, Principal Investigator). The authors would like to thank Gary Robb for assistance with the preparation of the apparatus and for the planning and deployment of the apparatus in the field, and Justin Dix for advice

REFERENCES

1. T. G. Leighton, A. D. Phelps, and D. G. Ramble, "Bubble detection using low amplitude multiple acoustic techniques," *Proceedings of the 3rd European Conference on Underwater Acoustics, Heraklion* (ed. J. Papadakis), pp. 1143-1147, 1996.
2. T. G. Leighton, D. G. Ramble, and A. D. Phelps, "The detection of tethered and rising bubbles using multiple acoustic techniques," *Journal of the Acoustical Society of America*, Vol. 101(5), pp. 2626-2635, 1997.
3. A. G. Judd, and M. Hovland, "The evidence of shallow gas in marine sediments," *Cont. Shelf Res.*, Vol. 12(10), pp. 1081-1095, 1992.
4. P. Fleischer, T. H. Orsi, M. D. Richardson, and A. L. Anderson, "Distribution of free gas in marine sediments: a global overview, Geo-Marine Letters, Vol. 21, pp. 103-122, 2001.
5. A. R. Tinkle, K. R. Wener, and C. A. Meeder, "Seismic no-data zone, offshore 1988, Mississippi delta: Part 1-Acoustic characterisation," *Proceedings to the 20th Offshore Technology Conference (Houston)*, pp. 65-74, 1988.
6. A. I. Best, M. D. J. Tuffin, J. K. Dix, and J. M. Bull, "Tidal height and frequency dependence of acoustic velocity and attenuation in shallow gassy marine sediments," *J. Geophys. Res*., Vol. 109, Art. No. B08101, 2004.
7. K. Andreassen, P. E. Hart, and M. MacKay, "Amplitude versus offset modelling of the bottom stimulated reflection associated with submarine gas hydrates," *Mar. Geol.*, Vol. 137, pp. 25-40, 1997.
8. F. K. Levin, "The seismic properties of Lake Maracaibo," *Geophysics*, Vol. 27, pp. 35-47, 1962.
9. M. P. Hochstein, "Seismic measurements in Suva Harbour (FIJI)," *New Zeal. J. Geol. Geophys*., Vol. 13, pp. 269-281, 1970.
10. G. H. Lee, D. C. Kim, H. J. Kim, H. T. Jou, Y. J. Lee, and S. C. Park, "Shallow gas off the southeastern cost of Korea," *Proceedings to the VIII International Conference on Gas in Marine Sediments (Vigo)*, pp. 87-89, 2005.
11. P. Hempel, V. Spiess, and R. Schreiber, "Expulsion of shallow gas in the Skagerrak-Evidence from subbotton profiling, seismic, hydroacoustic and geochemical data," *Estuar. Coast. Shelf Sci.*, Vol. 38, pp. 583-601, 1994.
12. T. S. Edrington, and T. M. Calloway, "Sound speed and attenuation measurements in gassy sediments in the Gulf of Mexico," *Geophysics*, Vol. 49, pp. 297-299, 1984.
13. J. L. Jones, C. B. Leslie, and L. E. Barton, "Acoustic characteristics of underwater bottom, *J. Acoust. Soc. Am.*, Vol. 36, pp. 154-157, 1964.
14. P. S. Wilson, A. H. Reed, W. T. Wood, and R. A. Roy, "Low frequency sound speed measurements paired with computed X-Ray tomography imaging in gas-bearing

reconstituted natural sediments," *Proceedings to the 2nd international conference on Underwater acoustic measurements: Technologies and Results (Heraklion)*, pp. 21-29, 2007.

15. B. S. Hart, and T. S. Hamilton, "High-resolution acoustic mapping of shallow gas in unconsolidated sediments beneath the strait of Geogia, British Columbia," *Geo-Mar. Lett*., Vol. 13, pp. 49-55, 1993.
16. J. L. Jones, C. B. Leslie, and L. E. Barton, "Acoustic characteristics of a lake bottom", *J. Acoust. Soc. Am*., Vol. 30, pp. 142-145, 1958.
17. A. B. Wood, and D. E. Weston, "The propagation of sound in mud," *Acustica*, Vol. 14, pp. 156-162, 1964.
18. S. S. Fu, R. H. Wilkens, and L. N. Frazer, "In situ velocity profiles in gassy sediments: Kiel Bay," *Geo-Marine Letters*, Vol. 16, pp. 249-253, 1996.
19. P. E. Keplay, and R. C. Cooke, "Velocity of sound as a function of bubble distribution in gas-bearing sediments," *Geophys. Res. Lett.*, Vol. 5, pp. 1071-1073, 1978.
20. S. K. Addy, and J. L. Worzel, "Gas seeps and subsurface structure off Panama city, Florida," *AAPG Bull.* Vol. 63, pp. 668-675, 1979.
21. T. J. Gorgas, R. H. Wilkens, S. F. Shung, L. N. Frazer, M. D. Richardson, K. B. Briggs, and H. Lee, "In situ acoustic and laboratory ultrasonic sound speed and attenuation measured in heterogeneous soft seabed sediments: Eel River shelf, California," *Mar. Geol.*, Vol. 182, pp. 103-119, 2002.
22. R. H. Wilkens, and M. D. Richardson, "The influence of gas bubbles on sediment acoustic properties: in situ, laboratory, and theoretical results from Eckernförde Bay, Baltic sea," *Cont. Shelf Res.*, Vol. 18, pp. 1859-1892, 1998.
23. T. N. Gardiner, "An acoustic study of soils that model seabed sediments containing gas bubbles," *J. Acoust. Soc. Am.*, Vol. 107, pp. 163-176, 2000.
24. W. L. Nyborg, I. Rudnick, and H.K. Schilling, "Experiments on acoustic absorption in sand and soil," *J. Acoust. Soc. Am.*, Vol. 22, pp. 422-425, 1950.
25. A. L. Anderson, and L. D. Hampton, "Acoustics of gas bearing sediments I, Background," *J. Acoust. Soc. Am*., Vol. 67, pp. 1865-1889, 1980.
26. H. Brandt, "Factors affecting compressional wave velocities in unconsolidated marine sand sediments," *J. Acoust. Soc. Am.*, Vol. 32, pp. 171-179, 1960.
27. L. D. Hampton, and A. L. Anderson, "Acoustics and gas in sediments: Applied Research Laboratory (ARL) experience," in *Natural gas in marine sediments*, edited by I.R. Kaplan, Plenum Press, New York, pp 249-273, 1974.
28. S. N. Domenico, "Effect of brine-gas mixture on velocity in an unconsolidated sand reservoir," *Geophysics*, Vol. 41, pp. 882-894, 1976.
29. S. N. Domenico, "Elastic properties of unconsolidated porous sand reservoirs," *Geophysics*, Vol. 42, pp. 1339-1368, 1977.
30. D. C. Kim, J. Y. Yeo, G. H. Lee, and S. C. Park, "Seismic characteristics and physical properties of gas-bearing sediment in the Jinhae Bay, the South Sea of Korea," *Proceedings to the VIII International Conference on Gas in Marine Sediments (Vigo)*, pp. 185-190, 2005.
31. F. Yuan, J. D. Bennell, and A. M. Davis, "Acoustic and physical characteristics of gassy sediments in the western Irish Sea," *Cont. Shelf Res*., Vol. 12, pp. 1121-1134, 1992.

32. N. C. Slowey, W. R. Bryant, and D. N. Lambert, "Comparison of high-resolution seismic profiles and the geoacoustic properties of Eckernforde Bay sediments," *Geo-Mar. Lett*., Vol. 16, pp. 240-248, 1996.
33. S. E. Elliot, and B. F. Wiley, "Compressional velocities of partially saturated unconsolidated sands," *Geophysics*, Vol. 40, pp. 949-954, 1975.
34. T. G. Leighton, "Theory for acoustic propagation in marine sediment containing gas bubbles which may pulsate in a non-stationary nonlinear manner, Geophysical Research Letters, Vol. 34, L17607, doi:10.1029/2007GL030803, 2007.
35. T. G. Leighton, "A method for estimating sound speed and the void fraction of bubbles from sub-bottom sonar images of gassy seabeds, ISVR Technical Report No. 320, University of Southampton, 2007.
36. T. G. Leighton, "Theory for acoustic propagation in solid containing gas bubbles, with applications to marine sediment and tissue, ISVR Technical Report No. 318, University of Southampton, 2007.
37. G. B. N. Robb, T. G. Leighton, V. F. Humphrey, A. I. Best, J. K. Dix, and Z. Klusek, "Investigating acoustic propagation in gassy marine sediments using a bubbly gel mimic, ISVR Technical Report 315, University of Southampton, 2007.
38. S. J. Wheeler, and T. N. Gardiner, "Elastic moduli of soils containing large gas bubbles," *Geotechnique*, Vol. 39(2), pp. 333-342, 1989.
39. G. C. Sills, S. J. Wheeler, S. D. Thomas, and T. N. Gardiner, "Behaviour of offshore soils containing gas bubbles," *Geotechnique*, Vol. 41(2), pp. 227-241, 1991.
40. A. G. Judd, "The global importance and context of methane escape from the seabed," *Geo-Marine Letters*, Vol. 23, pp. 147-154, 2003.
41. T. G. Leighton, and G. J. Heald, "Chapter 21: Very high frequency coastal acoustics," In: *Acoustical Oceanography: Sound in the Sea* (Cambridge University Press) (H. Medwin, editor), pp. 518-547, 2005.
42. T. G. Leighton, D. G. Ramble, and A. D. Phelps, "Comparison of the abilities of multiple acoustic techniques for bubble detection," *Proceedings of the Institute of Acoustics*, Vol. 17 (8), pp. 149-160, 1995.
43. T. G. Leighton, P. R. Birkin, M. Hodnett, B. Zeqiri, J. F. Power, G. J. Price, T. Mason, M. Plattes, N. Dezhkunov, and A. J. Coleman, "Characterisation Of Measures Of Reference Acoustic Cavitation (COMORAC): An experimental feasibility trial," in: Bubble and Particle Dynamics in Acoustic Fields: Modern Trends and Applications (A. A. Doinikov, editor) (Research Signpost, Kerala), pp. 37-94, 2005.
44. S. Vagle, and D. M. Farmer, "A comparison of four methods for bubble size and void fraction measurements," IEEE Journal of Oceanic Engineering, Vol. 23(3), pp. 211-222, 1998.
45. T. G. Leighton, A. D. Phelps, and D. G. Ramble, "Acoustic bubble sizing: From laboratory to the surf sone trials," *Acoustic Bulletin*, Vol. 21, pp. 5-12, 1996.
46. T. G. Leighton, A. D. Phelps, and D. G. Ramble, and D. A. Sharpe, "Comparison of the abilities of eight acoustic techniques to detect and size a single bubble," *Ultrasonics*, Vol. 34, pp. 661-667, 1996.
47. T. G. Leighton, M. D. Simpson, S. D. Meers, P. R. White, G. J. Heald, H. A. Dumbrell, J. W. L. Clarke, P. R. Birkin, and Y. Watson, "Abstract on: Surf-zone bubble detection using

multiple techniques: The Worbarrow Bay experiment," *Journal of the Acoustical Society of America*, Vol. 108(5), pp. 2493, 2000.

48. T. G. Leighton, S. D. Meers, M. D. Simpson, J. W. L. Clarke, G. T. Yim, P. R. Birkin, Y. E. Watson, P. R. White, G. J. Heald, H. A. Dumbrell, R. L. Culver, and S. D. Richards, "The Hurst Spit experiment: The characterization of bubbles in the surf zone using multiple acoustic techniques," *in 'Acoustical Oceanography', Proceedings of the Institute of Acoustics*, Vol. 23(2), pp. 227-234, 2001.
49. G. B. N. Robb, T. G. Leighton, V. F. Humphrey, A. I. Best, J. K. Dix, and Z. Klusek, "Investigating acoustic propagation in gassy marine sediments using a bubbly gel mimic," *Proceedings of the Second International Conference on Underwater Acoustic Measurements, Technologies and Results, Heraklion, Crete, Greece, 25-29 June*, pp. 31-38, 2007.
50. I. N. Didenkulov, S. I. Muyakshin, and D. A. Selivanovsky, "Bubble counting in the subsurface ocean layer," in *'Acoustical Oceanography', Proceedings of the Institute of Acoustics Vol. 23 Part 2*, T.G Leighton, G.J Heald , H. Griffiths and G. Griffiths, (eds.), Institute of Acoustics, pp. 220-226, 2001.
51. L. A. Ostrovsky, A. M. Sutin, I. A. Soustova, A. L. Matveyev, and A.I. Potapov, "Nonlinear scattering of acoustic waves by natural and artificially generated subsurface bubble layers in sea," *J. Acoust. Soc. Am.,* Vol. 113, pp. 741-749, 2003.
52. T. G. Leighton, "From seas to surgeries, from babbling brooks to baby scans: The acoustics of gas bubbles in liquids," *International Journal of Modern Physics B,* Vol. 18(25), pp. 3267-3314, 2004.
53. C. S. Clay, and H. Medwin, Acoustical Oceanography (Wiley, New York), 1977.
54. H. Medwin, and C. S. Clay, Fundamentals of Acoustical Oceanography, (Academic Press), 1998.
55. T. G. Leighton (editor), *Natural Physical Processes Associated With Sea Surface*, (publ. University of Southampton), 1997.
56. T. G. Leighton, G. J. Heald, H. Griffiths and G. Griffiths (editors), Acoustical Oceanography, Proceedings of the Institute of Acoustics Vol. 23 Part 2, (Bath University Press), 2001.
57. H. Medwin (editor) *Acoustical Oceanography: Sound in the Sea* (Cambridge University Press), 2004.
58. K. W. Commander, and A. Prosperetti, "Linear pressure waves in bubbly liquids: Comparison between theory and experiments," *J. Acoust. Soc. Am.*, Vol. 85, pp. 732-746, 1989.
59. W. K. Melville, E. Terrill, and F. Veron, "Bubbles and turbulence under breaking waves," in: *Natural Physical processes Associated with Sea Surface Sound* (ed. T.G. Leighton), University of Southampton, pp. 135-146, 1997.
60. H. A. Dumbrell, "Comparison of excess attenuation and backscatter measurements of ship wakes," in *Natural Physical processes Associated with Sea Surface Sound* (ed. T.G. Leighton) (University of Southampton), pp. 171-178, 1997.
61. E. J. Terrill, and W. K. Melville, "Broadband acoustic technique for measuring bubble size distribution: laboratory and shallow water measurements," *J. Atmos. Oceanic Technol.,* vol. 17, pp. 220-239, 1998.
62. R. Duraiswami, P. Sankar, and G.L. Chahine, "Bubble counting using an inverse acoustic scattering method," *J. Acoust. Soc. Am.,* vol. 104, pp. 2699-2717, 1998.

63. E. J. Terrill, G. Lada, and W. K. Melville, "Surf zone bubble populations," in *Acoustical Oceanography* (eds. T.G. Leighton, G.J. Heald, H. Griffiths and G. Griffiths), *Proceedings of the Institute of Acoustics*, Vol. 23 Part 2, Institute of Acoustics, pp. 212-219, 2001.
64. H. Medwin, "Counting Bubbles Acoustically: a Review," Ultrasonics, Vol. 1, pp. 7-13, 1977.
65. K. W. Commander, and R. J. McDonald, Finite-element solution of the inverse problem in bubble swarm acoustics. *J. Acoust. Soc. Am*. 89(2), pp. 592-597, 1991.
66. T. G. Leighton, S. D. Meers, and P. R. White, "Propagation through nonlinear time-dependent bubble clouds, and the estimation of bubble populations from measured acoustic characteristics," *Proceedings of the Royal Society A*, Vol. 460(2049), pp. 2521-2550, 2004.
67. T. G. Leighton, "What is ultrasound?" *Progress in Biophysics and Molecular Biology*, Vol. 93, Issues 1-3, pp. 3-83, 2007.
68. V. G. Welsby, and M. H. Safar, "Acoustic nonlinearity due to micro-bubbles in water," *Acustica*, Vol. 22, pp. 177-182, 1968/70.
69. E. A. Zablotskaya, and S. I. Soluyan, "Emission of harmonic and combination-frequency waves by air bubbles," *Phys. Acoust*., Vol. 18, pp. 396-398, 1973.
70. E. A. Zablotskaya, and S. I. Soluyan, "Nonlinear wave propagation in a liquid containing uniformly distributed air bubbles," *Phys. Acoust*., Vol. 19, pp. 442-444, 1974.
71. D. L. Miller, "Ultrasonic detection of resonant cavitation bubbles in a flow tube by their second-harmonic emissions," *Ultrasonics*, Vol. 19, pp. 217-224, 1981.
72. A. Yu. Sokolov, and A. M. Sutin, "Scattering of the second harmonic of an acoustic wave in a liquid containing gas bubbles," *Sov. Phys. Acoust.*, Vol. 29, pp. 59-61, 1983.
73. L. M. Kustov, V. E. Nazarov, and A. M. Sutin, "Nonlinear sound scattering by a bubble layer," *Sov. Phys. Acoust*., Vol. 32, pp. 500-503, 1986.
74. V. L. Newhouse, and P. M. Shankar, "Bubble size measurement using the nonlinear mixing of two frequencies," *J. Acoust. Soc. Am.*, Vol. 75, pp. 1473-1477, 1984.
75. V. A. Zverev, Yu. A. Kobelev, D. A. Selivanovski, and A. Yu. Sokolov, "Method of exposing gas bubbles in a fluid," *Sov. Phys. Tech. Phys.*, Vol. 25, pp. 897-898, 1980.
76. L. A. Ostrovsky, and A. M. Sutin, "Nonlinear sound scattering from subsurface bubble layers," in *Natural physical sources of underwater sound*, Kerman BR, ed. Kluwer academic publishers (Dordrecht, The Netherlands), pp. 363-370, 1993.
77. O. Ya. Butkovsky, E. A. Zablotskaya, Yu. A. Kravtsov, V.G. Petnikov, and V.V. Ryabikin, "Possibilities of active nonlinear spectroscopy of inhomogeneous condensed media," *Acta Phys. Slov.*, Vol. 36, pp. 58-63, 1986.
78. Yu. A. Ilinskii, and E. A. Zablotskaya, "Cooperative radiation and scattering of acoustic waves by gas bubbles in liquids," *J. Acoust. Soc. Am.* Vol. 92, pp. 2837-2841, 1992.
79. G. Du, and J. Wu, "Comparisons between two approaches for solvingnonlinear radiations from a bubble in a liquid," *J. Acoust. Soc. Am.* Vol. 87, pp. 1965-1967, 1990.
80. G. Du, and J. Wu, "Comments on "Comparisons between two approaches for solving nonlinear radiations from a bubble in a liquid"", *J. Acoust. Soc. Am.* Vol. 94, pp. 2446, 1993.
81. E. A. Zablotskaya, "Response to "Comparisons between two approaches for solving nonlinear radiations from a bubble in a liquid"", *J. Acoust. Soc. Am.*, Vol. 94, pp. 2448, 1993.

82. Z. Kluzek, I. A. Soustova, and A. M. Sutin, “Nonlinear incoherent scattering of acoustic waves by a bubble layer,” *Acoustical Physics*, Vol. 42, pp. 568-575, 1996.
83. S. V. Karpov, Z. Klusek, A. L.Matveev, A. I.Potapov, and A. M.Sutin, "Nonlinear interaction of acoustic waves in gas-saturated marine sediments," *Acoust. Phys.*, Vol. 42, pp. 464-470, 1996.
84. A. D. Phelps, and T. G. Leighton, “High resolution bubble sizing through detection of the subharmonic response with a two frequency excitation technique,” *Journal of the Acoustical Society of America*, Vol. 99, pp. 1985-1992, 1996.
85. C. Devin, “Survey of Thermal, Radiation, and Viscous Damping of Pulsating Air Bubbles in Water,” *J. Acoust. Soc. Am.*, Vol. 31(12), pp. 1654-1667, 1959.
86. A. I. Eller, “Damping Constants of Pulsating Bubbles,” *J. Acoust. Soc. Am.*, Vol. 47(5), pp. 1469-1470, 1970.
87. A. D. Phelps and T. G. Leighton, “Oceanic bubble population measurements using a buoy-deployed combination frequency technique,” *IEEE Journal of Oceanic Engineering*, Vol. 23(4), pp. 400-410, 1998.
88. A. M. Sutin, S. W. Yoon, E. J. Kim and I.N. Didenkulov. “Nonlinear acoustic method for bubble density measurements in water”, *J. Acoust. Soc. Am.*, Vol. 103 (5), pp. 2377-2384, 1998.
89. T. G. Leighton, “Acoustic bubble detection. I. The detection of stable gas bodies,” *Environmental Engineering*, Vol. 7, pp. 9-16, 1994.
90. P. M. Morse, and H. Feshbach, Methods of theoretical physics, McGraw-Hill, pp. 1495-1498, 1953.